

## Accumulated photon echo in semiconductor microcrystalline quantum dots

T. Kuroda and F. Minami

*Department of Applied Physics, Tokyo Institute of Technology, Meguro, Tokyo 152-8551, Japan*

K. Inoue

*Research Institute for Electronic Science, Hokkaido University, Sapporo 060-0182, Japan*

A. V. Baranov

*S. I. Vavilov State Optical Institute, 199034 St. Petersburg, Russia*

(Received 28 October 1997)

The nonlinear coherent emission of excitons in CuBr quantum dots was investigated using a phase-stabilized photon-echo technique. The echo signal was observed to be quite strong, with the emission efficiency being three orders of magnitude larger than that of II-VI semiconductor quantum wells. Time resolving of the echo signal confirmed that the strong nonlinear emission originates from the accumulation effect of the population grating due to the presence of the bottleneck state. Formation and decay kinetics of the population grating was analyzed by taking into account the light-induced deexcitation effect. [S0163-1829(98)51804-8]

Semiconductor quantum dots (QD's) of a size comparable to the exciton radius have unique electronic properties associated with the three-dimensional confinement effect. Since QD's are expected to provide a large optical nonlinearity,<sup>1,2</sup> a number of nonlinear optical experiments have been performed, which include optical bleaching measurements revealing an efficient phase-space filling effect<sup>3,4</sup> and other nonlinear carrier dynamics,<sup>5</sup> and luminescence measurements exhibiting the strong biexcitonic emission.<sup>6</sup> Although QD's are known to show strong nonlinear signals, the origin of the nonlinearity itself is still controversial. In the present paper, we report the results of a photon-echo (PE) experiment in CuBr microcrystalline QD's. The nonlinear emission efficiency is found to be quite large, typically three orders of magnitude larger than that of II-VI thin film materials of a similar optical density. It is confirmed that such a strong nonlinear emission originates from the significant accumulation effect of the PE generating process.

The CuBr QD's were embedded in a multicomponent silicate glass at 0.1 wt %. The spherical dots were grown by using a diffusion phase decomposition method from a supersaturated solid solution of the basic constituents under secondary heat treatment. The mean radius of 3.2 nm was determined from a small-angle x-ray measurement. In the experiment, we observed the time-integrated (TI) and time-resolved (TR) intensities of the PE signal generated by two or three separated femtosecond pulses; for the three-pulse PE, resonant pulses with wave vectors  $\mathbf{k}_1$ ,  $\mathbf{k}_2$ , and  $\mathbf{k}_3$  (denoted by pulse Nos. 1, 2, and 3, respectively) were incident on the sample, and the signal emitted in the direction of  $-\mathbf{k}_1 + \mathbf{k}_2 + \mathbf{k}_3$  was measured, whereas, for the two-pulse PE, the self-diffracted signal emitted into  $-\mathbf{k}_1 + 2\mathbf{k}_2$  was measured. As will be described later, a small fluctuation in the time delay between the excitation pulses significantly diminished the diffracted signal intensity. Thus we designed the optical delay so as to fix the relative phase between the pulses. For excitation, we used a second-harmonic beam of an output light from a mode-locked Ti-sapphire laser (76-

MHz repetition rate) producing pulses of 100-fs temporal duration and 28-meV spectral width. The beam was divided into two or three beams of equal intensity, and the intensity was varied from 0.2  $\mu\text{W}$  to 6 mW. To avoid the high-density effects, the excitation beam spot was defocused on the specimen so that the spot size was of  $\sim 0.2$ -mm diameter. The diffracted signals were detected by a photomultiplier tube connected to either a lock-in amplifier (data of Fig. 1) or a digitizing oscilloscope (Figs. 2-4) for the TI measurement, and a streak camera with a 4-ps time resolution for the TR measurement. The absorption spectrum of the QD's is plotted in the inset of Fig. 1 together with the spectrum of the excitation pulse. The lowest absorption peak is attributed to the  $S$  confinement state of the  $Z_{12}$  exciton, which is inhomogeneously broadened by the size distribution of the QD's. The laser wavelength was tuned to excite the lower-energy side of the  $Z_{12}$  exciton band so as to observe only the nonlinear response of the  $Z_{12}$  exciton by eliminating the contribution of the higher exciton states. All experiments were performed at 5 K.

In Fig. 1, an example of the TI intensity of the two-pulse PE signals is shown as a function of the time separation between pulse Nos. 1 and 2 ( $\tau_{12}$ ), where the excitation power density is 50  $\text{pJ cm}^{-2}$  per pulse. Due to the large nonlinear efficiency, we could obtain the PE signal by using such a weak excitation power, so that the influence of the exciton-exciton scattering is eliminated on the phase relaxation process. In this configuration, the homogeneous dephasing time  $T_2$  is determined as four times the observed decay time, because the absorption peak is inhomogeneously broadened. The signal is found to consist of two components with different decay times of 0.41 and 2.1 ps, yielding the dephasing times of 1.6 and 8.4 ps, respectively. This fact indicates that the dominant contribution to the PE signal comes from the two different transitions. The origin of the present split transitions is interpreted in terms of the zero-phonon exciton level and the LO-phonon-coupled exciton state. As was found in the spectral measurement,<sup>7</sup> the transi-

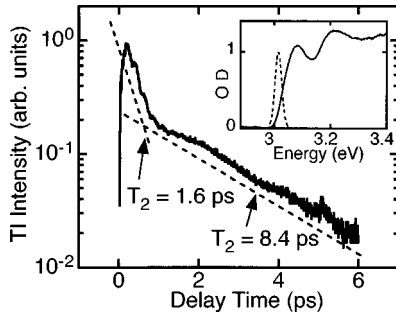


FIG. 1. TI intensity of the two-pulse photon-echo signal in CuBr quantum dots as a function of  $\tau_{12}$ . The excitation intensity for each beam is  $50 \text{ pJ cm}^{-2}$  per pulse. Spectra of the absorbance (solid line) and the excitation pulse (broken line) are also shown in the inset.

tion amplitude of the phonon-coupled level is comparable with that of the zero-phonon state, so that it should appear in the PE signal as the rapid decaying component. The dephasing time of the phonon-coupled exciton is in agreement with results of the size-selective spectral measurement, in which the homogeneous width is given by the linewidth of the resonant LO-phonon hyper-Raman signal.<sup>7,8</sup> The oscillatory feature seen in the early stage of the decay curve represents the quantum beats between the LO-phonon coupled states, the existence of which reflects the strong electron-phonon coupling in the QD's.<sup>9,10</sup>

The diffracted signals are very strong and easily visible to the naked eye even with weak excitation. In Fig. 2, the absolute TI intensity of the three-pulse PE signal is plotted as a function of the incident power, where  $\tau_{12}=0.6 \text{ ps}$ , and pulse Nos. 2 and 3 are overlapped ( $\tau_{23}=0$ ). Note that the signal can be resolved even with a sub- $\mu\text{W}$  excitation beam, and the dependence of the signal on the excitation power is linear. We found that the dephasing time is independent of the excitation power over the present range, so that the linear power dependence is not caused by the exciton-exciton scattering. To compare the emission signal with that of other semiconductor materials, we also observed the self-diffracted signals of 50 periods of 9.2-nm-thick ZnSe/ZnSSe quantum wells (QW's) under a similar excitation condition. We chose the ZnSe QW's since they possess almost the same optical density as the CuBr QD's. As seen in Fig. 2, the diffracted signal in the ZnSe QW's shows a cubic power dependence, and it is much weaker than that of the CuBr QD's. The difference in the emission efficiency between the QW's and QD's increases with decreasing incident power, and the signals of the QD's become three orders of magnitude larger than those of the QW's at the weakest excitation.

Observation of the strong nonlinear emission and the linear power dependence implies that the accumulated PE phenomenon is involved in the relevant optical process. It is known that the PE signal is enhanced by an accumulation effect of the population grating, when the system involves a very slow relaxation process caused by, e.g., the presence of a bottleneck state.<sup>11,12</sup> By grating, we mean a periodic distribution of the population of the ground and excited states as a function of energy. Due to the presence of the bottleneck state, the population grating is accumulated through the successive excitation with a pulsed laser of high repetition rate. The PE signal is, then, greatly enhanced by the scattering from the accumulated grating which is deeply modulated. It

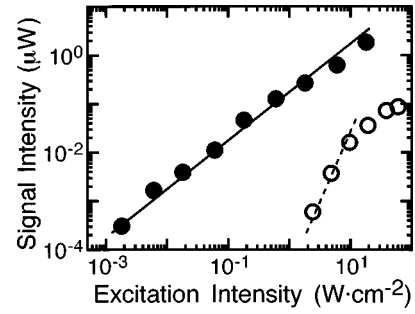


FIG. 2. The absolute intensity of the three-pulse PE signal with  $\tau_{12}=0.6 \text{ ps}$  and  $\tau_{23}=0$ , as a function of excitation power (filled circle). The self-diffracted signal of 50 periods of 92-A ZnSe quantum wells is also plotted (open circle). Linear and cubic dependences on the incident power are also indicated by solid and broken lines, respectively.

is important to note that this grating does not mean a transient *spatial grating* induced by two temporally overlapped pulses; the characteristic feature is observed even when the pulses are separated, and the accumulation process is independent of  $\tau_{12}$ . It is also noted that the PE intensity is very sensitive to a small phase fluctuation, since the formation of the accumulated PE requires a train of excitation pulses with a constant phase difference. Thus a stable optical system is quite necessary for an observation of this phenomenon.

A requisite for the accumulated PE (APE) is that the lifetime of the bottleneck level is longer than the pulse repetition time. The induced nonlinear polarization is roughly expressed as

$$P_{\text{APE}}^{(3)} = \frac{\nu_{\text{laser}} + \nu_b}{\nu_b} P_0^{(3)} \approx \frac{\nu_{\text{laser}}}{\nu_b} P_0^{(3)}, \quad (1)$$

where  $\nu_{\text{laser}}$  represents the repetition rate of the excitation pulses,  $\nu_b$  is the entire relaxation rate of the relevant system governed by the inverse of the bottleneck lifetime, and  $P_{\text{APE}}^{(3)}$  and  $P_0^{(3)}$  are the diffracted signals with and without the accumulation effect, respectively. In the present case, since  $\nu_b^{-1}$  is in the ms range, as will be described later, the nonlinear signal should be enhanced by  $10^3 - 10^6$ . It is noted that the presence of electronic states with such slow relaxation has also been reported by several authors, as the observation of a slow photoluminescence decay on a  $\mu\text{s}$  time scale,<sup>13</sup> and a long-lived bleaching with the time constant from  $\sim \mu\text{s}$  to several hours.<sup>14,15</sup> The microscopic origin of these long-lived phenomena is not yet well known. However, it is believed that these effects are closely connected to the carrier localization to the QD surface.<sup>4</sup>

To clarify that the slow relaxation process plays an essential role in the nonlinear emission, we also examined the formation kinetics of the population grating. In the upper part of Fig. 3, the evolution of the TI intensity of the two-pulse PE signal is shown, where beam No. 1 is modulated by an optical chopper, and beam No. 2 is unmodulated. When beam No. 1 is irradiated during  $t_1 \leq t \leq t_2$ , the population grating starts to accumulate from  $t_1$  and disappear from  $t_2$ . It is found that the echo signal still appears even when beam No. 1 is blocked. Such a memory effect of the population grating is directly observed by a time resolving of the PE signal, as seen in the lower part of Fig. 3. The echo signal is

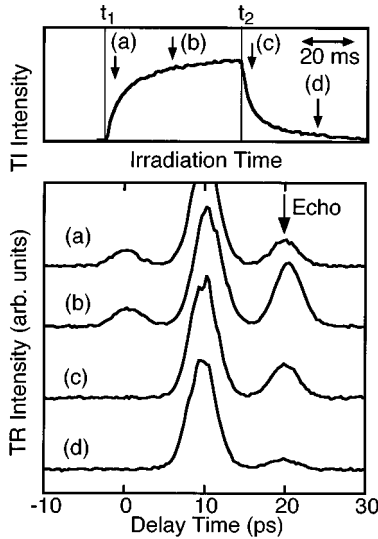


FIG. 3. (Top) Evolution of the TI intensity of the two-pulse PE signal with  $\tau_{12} = 10$  ps, where  $\tau_{12} = 10$  ps, and pulse No. 1 is modulated and irradiated during  $t_1 \leq t \leq t_2$  using an optical chopper of 10-Hz rate. The excitation intensity is  $80 \text{ mW cm}^{-2}$ . (Bottom) TR intensity of the same signal taken at a different irradiation time corresponding to (a)–(d) in the top figure. The signals observed at 0 and 10 ps represent the scattered light of the first and second pulses, respectively. The echo signal is found at  $\sim 20$  ps.

resolved at  $2\tau_{12} = 20$  ps, even when the first pulse is not irradiated [Figs. 3(c) and 3(d)]. This behavior indicates a preservation of the population grating, reflecting the slow relaxation process from the bottleneck state to the ground state.

The time evolution of the accumulated grating is calculated in terms of the Bloch equations for a system with a bottleneck level.<sup>12</sup> As a result, the development of the TI intensity of the accumulated PE signal is given by

$$I(t > t_1) \propto \{1 - \exp[-\nu_b(t - t_1)]\}^2, \quad (2)$$

$$I(t > t_2) \propto \exp\{-2\nu_b(t - t_2)\}. \quad (3)$$

This expression indicates that the evolution of the echo intensity is determined solely by the bottleneck lifetime. However, we experimentally found that both the decay rise times dramatically decrease with increasing excitation intensity, as shown in the inset of Fig. 4. This feature is interpreted in terms of the light-induced deexcitation effect; for strong (or even weak) excitation, electrons which fall into a bottleneck state are simultaneously deexcited to an excited electronic level. As a result, the population grating disappears more quickly, and the formation and decay characteristics of the grating are observed to be faster than the *pure* bottleneck relaxation process. To take into account the deexcitation effect,  $\nu_b$  in the above equations should be replaced by the *effective* bottleneck relaxation rate,  $\nu_b^{\text{eff}}$ , that is,

$$\nu_b^{\text{eff}} = \nu_b + \Gamma_{\text{deex}}, \quad (4)$$

where  $\Gamma_{\text{deex}}$  represents the deexcitation rate under irradiation. Since the deexcitation arises from the linear absorption pro-

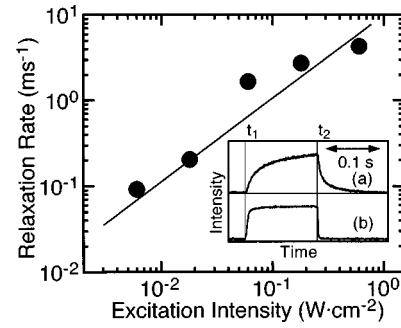


FIG. 4. Variation in the relaxation rate of the bottleneck state by varying the excitation intensity. The linear power dependence is represented by the solid line. Time evolutions of the three-pulse PE intensities for the different excitation powers of (a)  $6 \text{ mW cm}^{-2}$  and (b)  $0.6 \text{ W cm}^{-2}$  are also indicated in the inset, where  $\tau_{12} = 0.6$  ps and  $\tau_{23} = 0$ , and the modulation frequency of pulse No. 1 is 4 Hz.

cess from the bottleneck state,  $\Gamma_{\text{deex}}$  should linearly depend on the incident power. The magnitudes of  $\nu_b^{\text{eff}}$  obtained by fitting with Eqs. (2) and (3) are presented in Fig. 4, and show the linear intensity dependence, as expected. Moreover, the observed dependence suggests that the pure bottleneck lifetime is quite long, so that the bottleneck relaxation is mainly caused by the deexcitation process, i.e.,  $\nu_b \ll \Gamma_{\text{deex}}$ , even with the weakest excitation condition of the present experiment. This result suggests that the previously reported long-lived phenomena, which were on a wide range of the time scale from  $\sim \text{ns}$  to several hours,<sup>4,13–15</sup> should crucially depend on the excitation condition of each experiment, as well as on the intrinsic microscopic mechanism.

The deexcitation process is also responsible for the linear power dependence of the diffracted signal intensity shown in Fig. 2. As seen in Eq. (1), the nonlinear polarization of the accumulated PE is proportionally enhanced to the bottleneck lifetime, that is, the signal intensity  $|P_{\text{APE}}^{(3)}|^2$  is proportional to  $(\nu_b^{\text{eff}})^{-2} \approx (\Gamma_{\text{deex}})^2$ . Consequently, the degree of power dependence of the diffracted signal reduces to the first order, although the PE process is originally a third-order nonlinear optical process.

Finally, we would like to point out the possible mechanism which leads to the bottleneck effect. It is widely accepted that the long-lived phenomena of QD's arise from the decomposition of an exciton into an electron and a hole, either of which is captured to the surface. Due to this, the overlapping between the electron and hole decreases, reducing the recombination rate, and causing the bottleneck effect. It is therefore understandable that the deexcitation of the bottleneck level is the transition of the trapped carrier into the higher-excited delocalized state. The carrier recombination probability, thereby, increases with increasing excitation power, showing the rapid relaxation. However, further investigation is clearly needed to obtain a definite answer on the origin of the deexcitation effect.

In conclusion, we have presented an observation of the accumulation effect of the transient nonlinear optical response in semiconductor quantum dots. Using a phase-stabilized photon technique, we found that the nonlinear diffracted signal is greatly enhanced due to the presence of the bottleneck state of a very long lifetime. Due to the large

nonlinear emission efficiency, we could determine the dephasing time of the exciton under an extremely weak excitation condition. Our results demonstrate that the light-induced deexcitation effect dominates the relaxation process from the bottleneck state even with the weak excitation condition on the order of  $100 \mu\text{W cm}^{-2}$ . We confirmed that the accumulated PE experiment allows a direct investigation of

the entire relaxation dynamics involved in quantum dot systems.

The authors are grateful to Dr. Shuji Asaka for his valuable discussions. This work was supported by a Grant-in-Aid from the Ministry of Education, Science, Sports and Culture of Japan, and Special Coordination Funds for Promoting Science and Technology from STA of Japan.

- 
- <sup>1</sup>L. Banyai and S. W. Koch, *Semiconductor Quantum Dots* (World Scientific, Singapore, 1993).
- <sup>2</sup>E. Hanamura, *Phys. Rev. B* **37**, 1273 (1987).
- <sup>3</sup>A. P. Alivisatos, A. L. Harris, N. J. Levinos, M. L. Steigerwald, and L. E. Brus, *J. Chem. Phys.* **89**, 4001 (1988).
- <sup>4</sup>M. G. Bawendi, W. L. Wilson, L. Rothberg, P. J. Carroll, T. M. Jedju, M. L. Steigerwald, and L. E. Brus, *Phys. Rev. Lett.* **65**, 1623 (1990).
- <sup>5</sup>K. Edamatsu, S. Iwai, T. Itoh, S. Yano, and T. Goto, *Phys. Rev. B* **51**, 11 205 (1995).
- <sup>6</sup>Y. Masumoto, T. Kawamura, and K. Era, *Appl. Phys. Lett.* **62**, 225 (1993).
- <sup>7</sup>K. Inoue, A. Yamanaka, K. Toba, A. V. Baranov, A. A. Onushchenko, and A. V. Fedorov, *Phys. Rev. B* **54**, R8321 (1996).
- <sup>8</sup>T. Kuroda, S. Matsushita, F. Minami, K. Inoue, and A. V. Baranov, *Phys. Rev. B* **55**, R16 041 (1997).
- <sup>9</sup>D. M. Mittleman, R. W. Schoenlein, J. J. Shiang, V. L. Colvin, A. P. Alivisatos, and C. V. Shank, *Phys. Rev. B* **49**, 14 435 (1994).
- <sup>10</sup>T. Kuroda, F. Minami, K. Inoue, and A. V. Baranov, *Phys. Status Solidi A* **164**, 287 (1997).
- <sup>11</sup>W. H. Hesselink and D. W. Wiersma, *Phys. Rev. Lett.* **43**, 1991 (1979).
- <sup>12</sup>S. Asaka, H. Nakatsuka, M. Fujiwara, and M. Matsuoka, *Phys. Rev. A* **29**, 2286 (1984); *J. Phys. Soc. Jpn.* **56**, 2007 (1987).
- <sup>13</sup>M. Nirmal, C. B. Murray, and M. G. Bawendi, *Phys. Rev. B* **50**, 2293 (1994).
- <sup>14</sup>V. Esch, B. Fluegel, G. Khitrova, H. M. Gibbs, Xu Jiajin, K. Kang, S. W. Koch, L. C. Liu, S. H. Risbud, and N. Peyghambarian, *Phys. Rev. B* **42**, 7450 (1990).
- <sup>15</sup>K. Naoe, L. G. Zimin, and Y. Masumoto, *Phys. Rev. B* **50**, 18 200 (1994).